Astron. Astrophys. 311, 945–950 (1996)

ASTRONOMY AND ASTROPHYSICS

On the kinematics of the envelope of γ Cassiopeiae

Ph. Stee

Observatoire de la Côte d'Azur, Département Fresnel, CNRS URA 1361, 2130, route de l'Observatoire, Caussols, F-06460 St Vallier de Thiey, France

Received 25 October 1995 / Accepted 3 January 1996

Abstract. We study the rotational component of the wind in the envelope of the Be star γ Cas. We have computed scenarios based on the axi-symmetric radiative wind model that we have developed for this star. We obtain line profiles and predicted interferometric observables from long baseline Michelson interferometry. It turns out that the models with constant and solid body rotation can be ruled out. It is also shown that classical technics as spectroscopy as well as interferometry can not distinguish between the angular momentum conservation (β = 1.0), the Keplerian motion (β = 0.5) and β = 0.25 models. Besides, we have computed theoretical photocenter displacement as a fuction of wavelength in the North-South and East-West directions and also in the sky plane. We conclude that only technics which are able to follow the photocenter displacement with wavelength, as Michelson spectro-interferometry or differential speckle interferometry would be able to infer the actual rotational law in the envelope of γ Cas.

Key words: circumstellar matter – stars: individual: γ Cas – stars: imaging – stars: rotation

1. Introduction

Most of the studies which investigate the circular velocity laws in Be star envelopes are based on the observed equivalent width and the peak separation of emission profiles of HI and Fe II lines (Hanuschik et al. 1988; Hanuschik 1989; Dachs et al. 1992). Nevertheless Stee & Araujo (1994) have shown that using the peak separation of emission lines in order to determine the extent of the emitting region can lead to very large errors when a line-driven wind is present. In a recent paper Stee et al. (1995a, hereafter Paper I) present a possible scenario for the Be star γ Cas based on a radiative wind model. They obtained a good agreement between the model and spectroscopic, photometric and interferometric data collected with the GI2T (Mourard et al. 1994) stellar interferometer. In order to reproduce both the spectroscopic and interferometric measurements Stee et. al proposed a model in which the polar regions are dominated by optically thick lines whereas the equatorial regions are dominated by optically thin lines. In this scheme the inner equatorial regions, i.e close to the star, where most of the Hα emission originates, are dominated by the circular velocity, which was assumed to be Keplerian. More recently Araújo (1995) found that the rotational velocity must be close to a Keplerian law in order to obtain numerical solutions for the radial motion equation in the equatorial plane of rotating B-type stars. Other models often used the conservation of the angular momentum per unit of mass (Boyd & Marlborough 1991; Chen & Marlborough 1994). In this paper we investigate the possibility to use spectroscopic and spectrally resolved interferometric measurements in order to constrain the circular velocity law in the envelope of the Be star γ Cas.

In the present work we have adopted the following approach. First the starting point of the current study is based on what we have called our "best" model (BM) for γ Cas presented in Paper I, which gives a good spectroscopic and interferometric agreement between our model and the data obtained with the GI2T optical interferometer. We recall that the assumed rotational velocity field is given by:

$$v_\phi(r,\theta) \propto sin\theta\left(\frac{R}{r}\right)^\beta. \quad (1)$$

In order to study the dependence of model predictions on various β laws, we keep all the other parameters invariant except the β parameter.
We have computed five models:

- Constant rotation (β = 0.)
- β = 0.25 (a value used in Araújo et al. 1994)
- Keplerian motion (β = 0.5),
- Angular momentum conservation (β = 1.0),
- Solid body rotation (β = -1.0).

For each model we obtain the corresponding Hα line profile, the visibility and the apparent motion of the photocenters for different Doppler-shifts across Hα.

The remainder of this paper is organized as follows. In Sect. 2 we summarize the basic hypothesis and results of the BM

Send offprint requests to: stee@rossini.obs-nice.fr

used to build up a possible scenario for γ Cas. In section 3 we examine the effect of changing the β parameter on predicted Hα line profiles. Sect. 4 presents the corresponding visibility curves as a function of wavelength and baseline. In Sect. 5 we examine how the kinematics can affect the displacement of the photocenter at different Doppler-shifts across Hα. In the last section we summarize the main results of our study.

2. The model used for γ Cas

Our main hypothesis is that the envelope is axi-symmetric with respect to the rotational axis. No meridian circulation is allowed. We assume that the physics of the polar regions is well represented by a CAK type stellar wind model and the solutions for all stellar latitudes are obtained by introducing a parametrized model which is constrained by the data from the GI2T. The envelope is assumed to be formed by pure hydrogen atoms which have six bound levels. We have computed the ionization-excitation equation in the Sobolev approximation. The basic assumptions and equations of the model are given in detail in Paper I.

From a detailed reconstruction of the Hα profile and visibility curve we obtain an average equatorial terminal velocity of $V_\infty \sim 200$ km s^{-1} and an equatorial mass flux of $\Phi \sim 5 \cdot 10^{-8} M_\odot$ yr^{-1} sr^{-1}. This terminal velocity is obtained by introducing an optically thin line driven wind model in the equatorial regions of γ Cas. In order to obtain a good agreement with the observed data we have to provide the contribution of these weak lines to be about ten times greater than the force produced by the free electrons. The total mass loss rate is $\dot{M} = 3.2 \cdot 10^{-7} M_\odot$ yr^{-1} and agrees well with those given by Lamers and Waters (1987) who found $\dot{M}$ between $2.5 \cdot 10^{-8}$ and $5 \cdot 10^{-7} M_\odot$ yr^{-1} for γ Cas. We finally found that 90% of the Hα emission originates from an ellipsoid with a ratio of minor to major axis of 0.72. This major axis is about 17 stellar radii which corresponds to ~ 4 mas assuming a photosphere diameter of 0.45 mas. The major parameters used and the main results are summarized in Table 1.

Table 1. Parameters and results for γ Cassiopeiae

Parameters	
Spectral type	B0.5IVe
Effective temperature	25000 K
Mass	16 $M_\odot$
Radius	10 $R_\odot$
Stellar angular diameter	0.45 mas
Luminosity	$3.510^4 L_\odot$
Vsin i	230 km^{-1}
Inclination angle i	45°
Results	
Polar terminal velocity	2016 km s^{-1}
Polar mass flux	$1.7 \cdot 10^{-9} M_\odot$ yr^{-1} sr^{-1}
Equatorial terminal velocity	200 km s^{-1}
Equatorial mass flux	$5.1 \cdot 10^{-8} M_\odot$ yr^{-1} sr^{-1}
Mass loss rate	$3.2 \cdot 10^{-7} M_\odot$ yr^{-1}
Hα major axis	17 stellar radii
Hα oblateness	0.72
Hα extension	4 mas

3. Hα line profiles

We have solved the ionization-excitation equations (Sobolev 1960, Stee & Araújo 1994)

$$n_i\Big(\sum_{k=1}^{i-1} A_{ik}\beta_{ki} + B_{ic}\rho_{ic}\Big) = \sum_{k=i+1}^{\infty} n_k A_{ki}\beta_{ik} + n_e^2 C_i(T_e)\,, \quad (2)$$

where the escape probability is given by:

$$\beta_{ik} = \frac{1}{4\pi}\int \beta_{ik}^o (1 - e^{-1/\beta_{ik}^o}) d\Omega \quad (3)$$

with

$$\beta_{ik}^o = \frac{1}{2u}\frac{dv}{ds}\frac{1}{\alpha_{ik}}\,, \quad (4)$$

In order to take less computational time we have assumed that the density of the ionizing radiation to be constant and only diluted by the geometrical effect, i.e. we have not take into account continuum opacity effect. Anyway the small continuum opacity of the envelope produces only minor changes on the Hα line profiles and is independent of the envelope kinematics. Therefore the radiation density in Eq. (2) is given by:

$$\rho_{ic} = W\rho_{ic}^\star \quad (5)$$

where W is the dilution coefficient:

$$W = \frac{1}{2}\Big(1 - \sqrt{1 - (\frac{R}{r})^2}\Big) \quad (6)$$

and $\rho_{ic}^\star$ is the radiation density beyond the ith series at the surface of the star and R is the stellar radius. The other parameters in the ionization-excitation equation are the usual ones. More details can be found in Stee & Araújo (1994).

Fig. 1 shows the line profiles obtained for different values of the β parameter, i.e β=0., β=0.25; β=0.5; β=1.0; β=-1.0. The case of solid body rotation (β=-1.0) produces an absorption line profile and can easily be ruled out. The constant rotation (β=0.) case produces a more pronounced asymmetric double-peaked shape and a full width at half maximum (FWHM) which is twice the width of the Keplerian case. We recall that in the BM the rotational velocity law was assumed to be Keplerian (see Paper I). The cases with β=0.25 and the angular momentum conservation produce two line profiles with a shape very similar to the Keplerian one. For β=0.25 the intensity is 8 % smaller and the FWHM is 17 % larger whereas the β=1.0 case shows a strictly identical FWHM but an intensity 8 % larger than the Keplerian case.

From a purely spectroscopic point of view it is difficult to distinguish between the β=0.25; β=0.5 and β=1.0 models. With

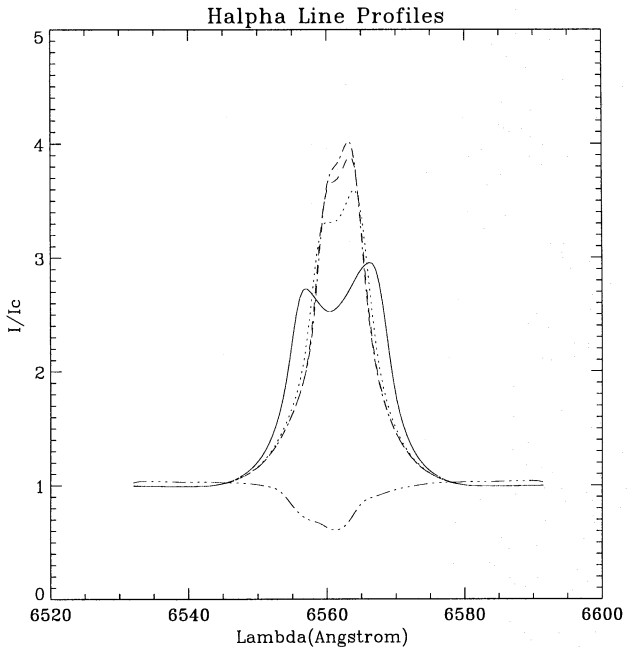

Fig. 1. Hα line profiles. Solid line: β=0., dotted: β=0.25, dashed: β=0.5,dash dot line: β=1.0, dash dot dot dot: β=-1.0

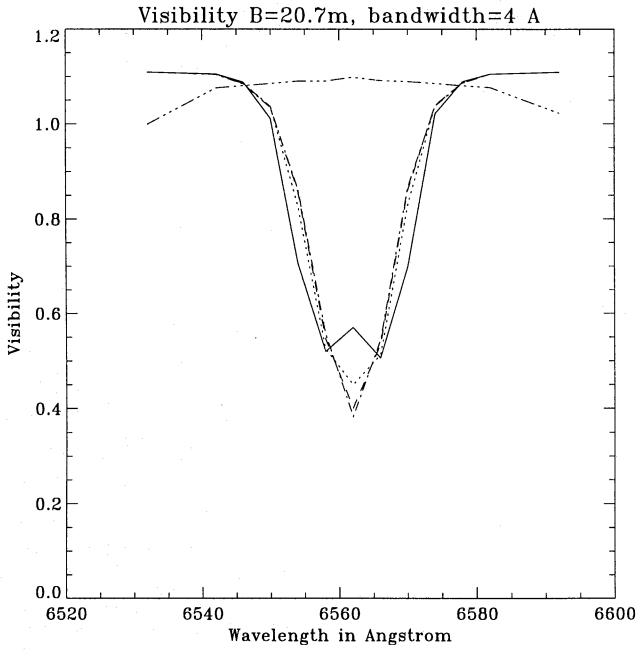

Fig. 2. Visibility measurement across the Hα line profile for the 20.7 meter baseline. Each visibility point is taken within a 4 AA bandwidth. Solid line β=0., dotted: β=0.25, dashed: β=0.5,dash dot line: β=1.0, dash dot dot dot: β=-1.0

two different β laws we may obtain a good agreement with the observed Hα line profile, without changing greatly the values of the computed visibilities, by just changing in our modelling another parameter, for instance the variation of the mass flux from the pole to the equator (the m1 parameter in Paper I).

4. Visibility curves as a function of wavelength and baseline

In order to study if interferometric measurements can add new constraints on the velocity laws we have computed for each model, 13 Doppler-shifted intensity maps, in a bandwidth of 4 AA, across the Hα line profile. The measured visibility by the GI2T corresponds to the ratio of the visibility in Hα to the visibility in the nearby continuum. Therefore, in order to compare our model with the data we have computed the intensity maps in the line and in the continuum. The continuum emission was computed by taking into account free-free and free-bound emissions and absorption mechanisms due to free-free and scattering. The resulting continuum emission is strictly identical to those obtain from the BM. We just recall that the envelope contribution to the continuum represents 17% of the total flux.

In order to compare our models with the data, we Fourier transform these maps independently and compute the ratio of the visibilities for 13 spatial frequencies across Hα. Fig. 2 displays the theoretical visibilities for different β laws at the 20.7 meter baseline.

As for the line profiles, we can immediately discard the case of β=-1.0 which results in a plateau with a maximum visibility at the central wavelength of Hα, i.e 6562 AA. This is due to the fact that the circular velocity is increasing with increasing distance from the stellar surface and by a Doppler effect shifts the envelope emission in the line above the Hα domain. So, the object appears more resolved, i.e more extended, in the continuum than in the Hα line. The constant rotation case produces a visibility curve which looks like more the observed one (see Paper I) but with a central reversal of the visibility at 6562 Å. As it can be seen in paper I, this feature is not observed. Thus, as from the study of the line profiles, the case of constant rotation may be ruled out.

For the three last β laws the visibility curves are quite similar. For instance, the visibility maximum difference between the Keplerian and the momentum conservation case, which occurs at 6562 Å, is less than 5 %. Fig. 3 depicts the effect of increasing the baseline of the interferometer, i.e the angular resolution. With the 37,8 meter baseline the visibilities are, of course, globally smaller (the object is more resolved), but the differences are still very small. The larger difference between the Keplerian and the momentum conservation case, is increasing but remains less then 6 %.

For the β=0., β=0.25, β=0.5 and β=1.0 cases we have also investigated the effect of reducing the bandwidth on the visibility curves. From Fig. 4 it appears that the shape of the curves does not change but the difference between the Keplerian and the momentum conservation case is increasing up to 7.5 % for the 37.8 meters baseline. Nevertheless, these differences are, at the present time, on the order of the uncertainties in the measured visibility points. Thus the visibility curves seem unable to distinguish between the β=0.25, β=0.5 and β=1.0 cases but confirm the result, from the line profiles study, that the constant and solid body rotation laws can be ruled out for γ Cas.

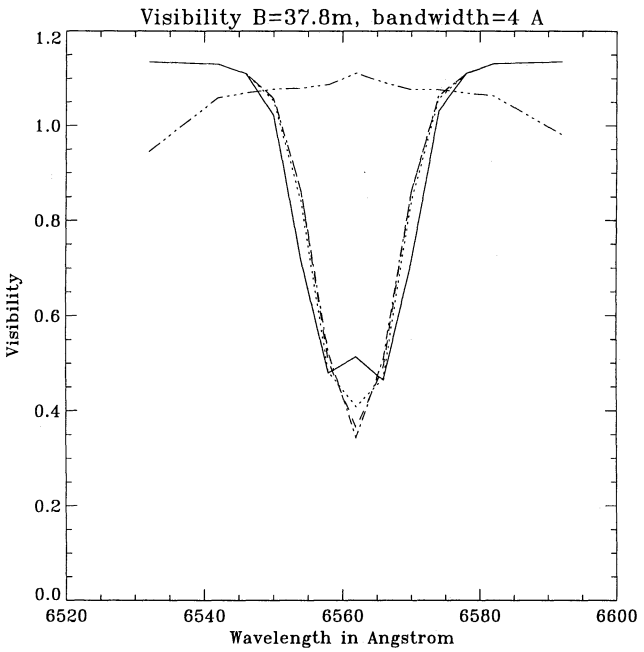

Fig. 3. Visibility measurement across the Hα line profile for the 37.8 meter baseline. Each visibility point is taken within a 4 AA bandwidth. Solid line: β=0., dotted: β=0.25, dashed: β=0.5,dash dot line: β=1.0, dash dot dot dot: β=-1.0

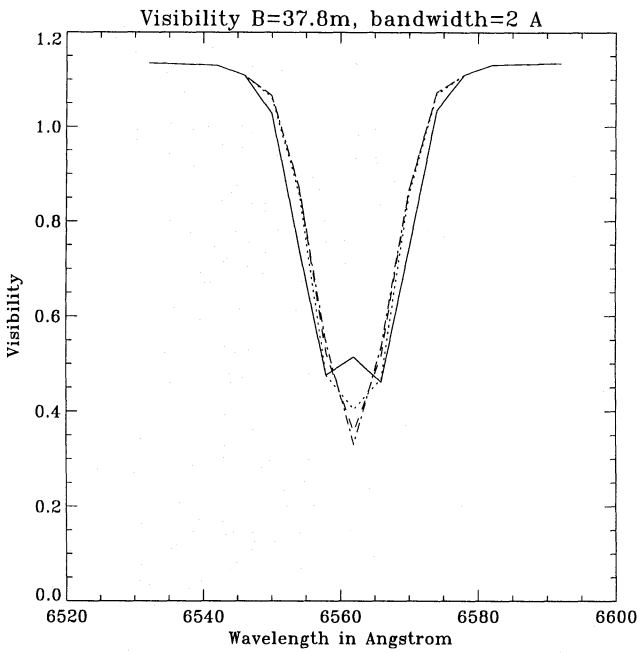

Fig. 4. Visibility measurement across the Hα line profile for the 37.8 meter baseline. Each visibility point is taken within a 2 AA bandwidth. Solid line: β=0., dotted: β=0.25, dashed: β=0.5,dash dot line: β=1.0, dash dot dot dot: β=-1.0

5. Effect of the kinematics on the photocenter displacement

As already emphasized in Paper I, Michelson spectro-interferometry gives us the modulus of the visibility but also the relative phase between the two channels which are cross-correlated (see also Stee et al. 1995b). For an unresolved source this relative phase is directly related to the photocenter displacement of the object in the corresponding channels. Due to the fact that we have not yet calibrated the phase visibility obtained with the GI2T, we have not presented a comparison between the theoretical photocenter displacement from our model and the GI2T data.

Nevertheless, other technics, as differential speckle interferometry (Beckers 1982) can also provide the displacement of the object photocenter with wavelength (Petrov 1989). As we will now see this photocenter shift is very sensitive to the β law used in the modelling. In Fig. 5 is shown the theoretical shift of the photocenter in the North-South direction for the β=0., β=0.25, β=0.5 and β=1.0 cases. The reference of the photocenter displacement, i.e. the zero of the shift, is given by the photocenter position of the continuum emission. Each map from which the photocenter is calculated is taken in a bandwidth of 4AA across Hα.

We notice that the photocenter displacement is increasing with decreasing β. We have made the same calculation but in the perpendicular direction, i.e in the East-West direction. From Fig. 6 it can be seen that the amplitude of the shift is smaller and that the differences between the models are not so well marked. For β=0., β=0.25, β=0.5 and β=1.0 the photocenter shifts respectively to $\pm$ 7.75, 5.60, 3.00 and 0.95 mas in the North-South direction. For the East-West direction the shift is respectively 3.92, 3.04, 2.76 and 2.65 mas. The wavelength at which the shift is maximum is 6558 Å and 6566 Å (symmetric to the Hα central wavelength) for the North-South case. For the East-West case it occurs at 6554 Å and 6570 Å.

The shape of the photocenter displacement is also different. For the North-South case it is first decreasing smoothly (this effect is more pronounced with larger β), then it is rapidly increasing up to the maximum value and it decreases down to zero. The rest of the displacement is symmetric with respect to zero. The East-West displacement is more complicated: first it decreases down to the minimum value, then it increases up to the 6554 Å wavelength, after it decreases down to zero (the slope is more important with increasing β) except for the β=0. case where the photocenter never stops increasing. The rest of the displacement is also symmetric with respect to zero. This symmetry is due to the fact that our model is axi-symmetric with respect to the rotational axis of the star. Finally the shift of the photocenter in the sky plane is shown in Fig. 7. The North is at the bottom and the East at the left of the map. From this figure we can notice that the surface of the sky covered by the photocenter displacement is increasing with decreasing β law. The photocenter is essentially moving along the rotation axis for β=1.0, and starts to move in the perpendicular direction for decreasing β. The main results are summarized in Table 2.

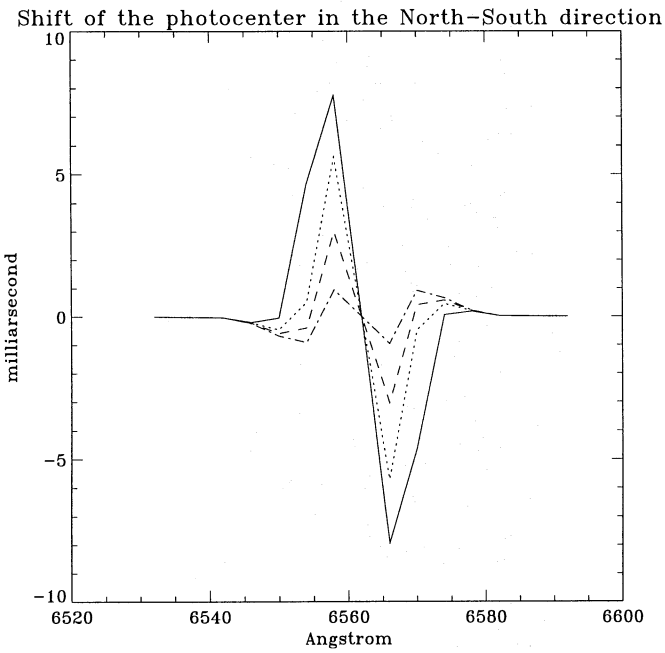

Fig. 5. Shift of the photocenter in the North-South direction. Each visibility point is computed within a 4 AA bandwidth. Solid line: β=0., dotted: β=0.25, dashed: β=0.5,dash dot line: β=1.0

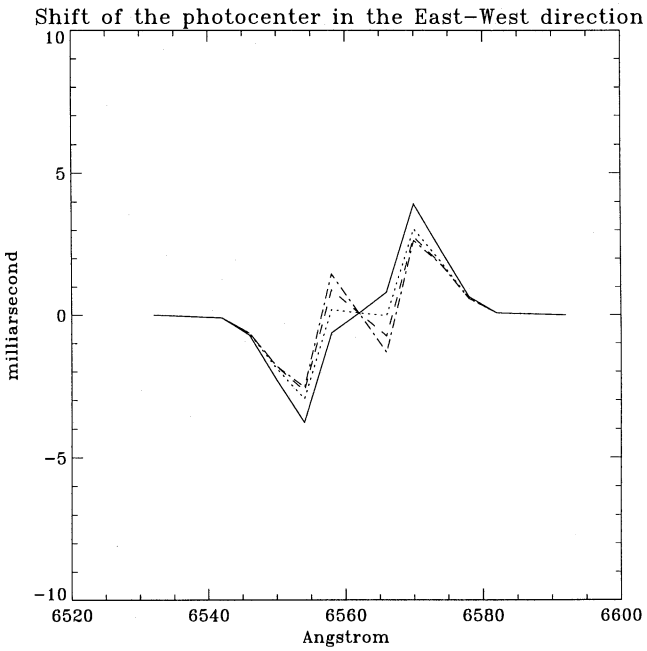

Fig. 6. Shift of the photocenter in the East-West direction. Each visibility point is computed within a 4 AA bandwidth. Solid line: β=0., dotted: β=0.25, dashed: β=0.5,dash dot line: β=1.0

Table 2. Shift of the photocenter as a function of the baseline direction and β law

Baseline direction	β	Maximum of the shift (in mas)	Corresponding λ of the shift
N-S	0.0	$\pm$ 7.75	6558 & 6566 Å
N-S	0.25	$\pm$ 5.6	6558 & 6566 Å
N-S	0.5	$\pm$ 3.00	6558 & 6566 Å
N-S	1.0	$\pm$ 0.95	6558 & 6566 Å
E-W	0.0	$\pm$ 3.92	6554 & 6570 Å
E-W	0.25	$\pm$ 3.04	6554 & 6570 Å
E-W	0.5	$\pm$ 2.76	6554 & 6570 Å
E-W	1.0	$\pm$ 2.63	6554 & 6570 Å

6. Summary and conclusion

By considering different β laws in the envelope of γ Cas we have shown that both Hα line profiles and visibility curves have rejected a constant or solid body rotation. Nevertheless, it is very difficult with these technics to distinguish between the momentum conservation, the Keplerian and a β=0.25 circular velocity law. Moreover, we recall that we have used the Sobolev approximation in our modelling. It is not obvious that this approximation applies in the equatorial regions where the rotation dominates, especially for the constant rotation case. Nevertheless, even if the rotational velocity gradient is zero, the radial component of the stellar wind velocity produces a non negligible photon escape probability in these regions. It can be objected that, depending on the choice of the radial expansion law, for some regions the velocity would weakly vary as a function of the distance from the star. In those cases, the Sobolev approximation can hardly be justified. Actually this situation occurs after about ten stellar radii, where the flow has reached its terminal velocity. This can change the shape of the line profiles at large Doppler shifts, especially in the line wings. On the other hand, in paper I we found that 90 % of the Hα emission originates within 17 stellar radii, where the Sobolev approximation correctly applies. Therefore, the computed visibility curves in Fig. 2, 3 and 4 remain valid. Finally the line profiles and the visibility curves allow a range of 0.2 - 1.0 for the β parameter. The keplerian case is in the middle of this range but we cannot, at the present time, discard other laws.

The only techniques which seem able to select the right rotational law are Michelson spectro-interferometry or differential speckle interferometry, which follow the shift of the photocenter with wavelength. In order to provide them theoretical observables, we have computed the displacement of the photocenter in the North-South, East-West and in the sky plane directions. This displacement is very sensitive to the circular velocity law and will be confronted with differential speckle interferometry data obtained by Petrov et al. 1995 (private communication) with the 2 meter telescope at the Observatoire de Haute Provence.

Acknowledgements. I thank D. Mourard and F.X. de Araújo who strongly encourage me in doing this work. I greatly acknowledge F. Vakili for many discussions and the careful reading of the manuscript. I am grateful to A.M. Hubert and D. Bonneau for their remarks. I also thank R. Petrov for fruitful discussions on the differential speckle interferometry technics. The useful remarks of the referee J. M. Marlborough are also greatly acknowledged by the author.

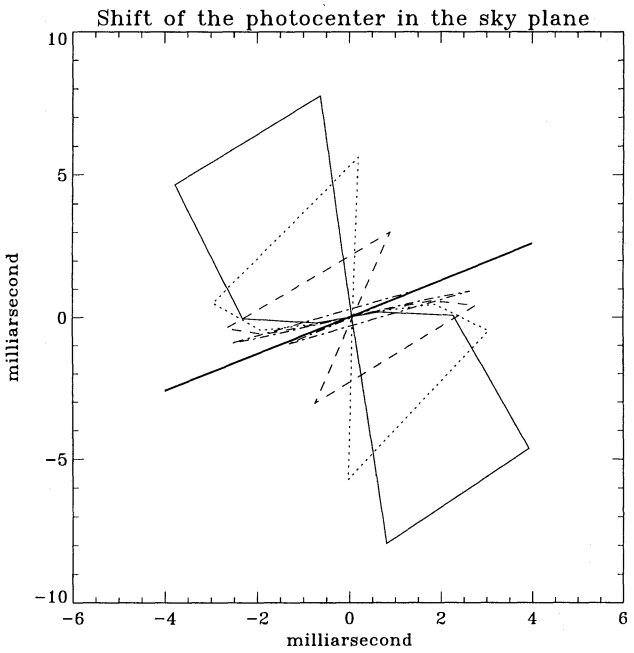

Fig. 7. Shift of the photocenter in the sky plane. The solid thick line is the direction of the rotation axis. Each visibility point is computed within a 4 AA bandwidth. Solid line: β=0., dotted: β=0.25, dashed: β=0.5,dash dot line: β=1.0

References

Araujo, F.X., Freitas Pacheco, J.A., Petrini, D. 1994, MNRAS, 267, 501
Araujo, F.X. 1995, A&A , 298, 179
Beckers, J.M. 1982, Opt. Acta, 29, 361
Boyd, C.J. and Marlborough, J.M. 1991, ApJ, 369, 191
Chen, H., and Marlborough, J. M. 1994, ApJ, 427, 1005
Dachs, J., Hummel, W. and Hanuschik R.W. 1992, A&AS, 95, 437
Hanuschik, R.W., Kozok, J.R., Kaiser, D. 1988, A&A, 189, 147
Hanuschik, R.W. 1989, Ap&SS, 161,61
Mourard, D., Bosc, I., Blazit, A., Bonneau, D.,Merlin, G., Morand, F., Vakili, F., Labeyrie, A. 1994, A&A , 283, 705
Petrov, R. G. 1989, in Proc. NATO ASI on Diffraction limited imaging with very large telescopes, Cargese, corse. Eds. J.M. Mariotti and D.M. Alloin, 249
Stee, Ph., and Araujo, F.X. 1994, A&A , 292, 221
Stee, Ph., de Araujo, X.F., Vakili, F., Mourard, D., Bonneau, D., Bosc-Tallon, I., Morand, F., Lawson, P. and Arnold, L., 1995a, Paper I, A&A, 300, 219
Stee, Ph., Bonneau D., Lawson, P., Morand, F., Mourard, D., Tallon, I., Vakili, F. 1995b, in Proc. ASP Conference Series, Eds. Comte, G. and Marcelin, M., Vol 71, 365
Sobolev, V.V. 1960, Moving envelopes of star, Harvard University Press, Cambridge, Mass.

This article was processed by the author using Springer-Verlag LaTeX A&A style file version 3.